Lattice Gases with Static Disorder: Renormalization of Mean Field Theory

A. J. H. Ossendrijver,[1] **A. Santos,**[2] **and M. H. Ernst**[1]

Lattice gas automata are used to model transport phenomena in random media with static disorder. If the interactions are repulsive, there is a large probability of backscattering or retracing collision sequences. In that case the Boltzmann equation or mean field theory breaks down, even in the limit of a low concentration of scatterers. Here sequences of uncorrelated and retracing collisions are of equal importance. The repeated ring approximation is used to resum the retracing trajectories, and the renormalized transport coefficients are calculated in the low-density limit, not only for hard core scatterers (diamonds, hexagons, triangles), but also for mixed point scatterers (mirrors, rotators, reflectors). The results are compared with extensive computer simulations.

1. INTRODUCTION

Percolation and transport phenomena in random media with static disorder are frequently modeled on lattices.[1-3] In most cases of physical interest the scatterers exert some short-range repulsion on the moving particles (backscattering). Due to the discrete nature of phase space, backscattering in lattice gases of arbitrary dimensionality introduces one-dimensional pathologies. A dramatic consequence is that the Boltzmann or mean field theory does not give the correct low-density behavior of such lattice gases, as first observed in refs 2 and 4. The effect of backscattering is particularly strong in the low-density limit, where the phase space accounting for uncorrelated collision sequences is equally large as the phase space

---

[1] Institute for Theoretical Physics, University of Utrecht, NL-3508 TA Utrecht, The Netherlands.
[2] Departamento de Física, Universidad de Extremadura, E-06071 Badajoz, Spain.

accounting for all retracing trajectories with returns to the same scatterer. This effect may reduce the transport coefficient by a factor on the order of two.[2]

In Lorentz models on square lattices with point scatterers the effective medium approximation gives predictions for the diffusion coefficient that agree well with the results of computer simulations at all densities.[2] Van Beijeren and Ernst have extended these results to an arbitrary number of dimensions and to arbitrary lattices.[5] Using an exact enumeration method for retracing trajectories, they have derived *exact* expressions for transport coefficients in the limit as $\rho \to 0$, and a simple *approximate* expression for all densities that agrees very well with the predictions of the more complex formulas of ref. 2. Unfortunately the theory of ref. 5 is only applicable to systems of *identical point* scatterers. The effective medium theory of ref. 2 does apply to mixtures of point scatterers, but can only be evaluated numerically.

The goal of the present paper is an analytic calculation of correlation functions and transport properties not only for identical point scatterers, but also for finite-size scatterers and mixtures of scatterers. In particular we focus attention on *low concentrations* of scatterers, because in such systems the backscattering events to be analyzed in the present paper are the *only* corrections to mean field theory. Here we propose an approximate resummation technique for lattice Lorentz gases that only accounts for the so-called repeated ring collisions, which form a subset of all retracing trajectories, and we present applications to several types of models. As an analytical test on the quality of this approximation we apply the theory to Lorentz gases with identical point scatterers and show that the resulting diffusion coefficient coincides with that obtained from the exact enumeration method. For random mixtures of point scatterers (e.g., right and left mirrors[3]) and for extended scatterers[6, 7] the resulting low-density diffusion coefficient is only approximate. Our analytic results are compared with computer simulations.

The plan of the paper is as follows: The necessary definitions and the microdynamic equations are introduced in Section 2. Section 3 describes the repeated ring approximation, which is solved analytically in Section 4 in the low-density limit. Section 5 shows that the repeated ring approximation is exact for identical point scatterers, and Section 6 compares the theoretical results for the diffusion coefficient with computer simulations. Some details on applications to random mixtures of point scatterers and to finite-size scatterers are given in appendices. The paper ends with a brief discussion.

2. LATTICE LORENTZ GAS

We consider a Lorentz gas on a regular d-dimensional space lattice $\mathcal{L}$ with $V = L^d$ sites, a coordination number equal to b, unit lattice distance, and periodic boundary conditions. A random fraction of the sites is occupied by a fixed scatterer. The configuration of scatterers is given by the set of occupation numbers $\mathbf{s} = \{s_a(\mathbf{r}); \ \mathbf{r} \in \mathcal{L}\}$, where $s_a(\mathbf{r}) = 1$ if site $\mathbf{r}$ is occupied by a scatterer of type a and $s_a(\mathbf{r}) = 0$ otherwise. The expectation value $\langle s_a(\mathbf{r}) \rangle = \rho_a$ denotes the density of scatterers of type a, where the average is taken over a site-independent distribution of scatterers. The total density of scatterers is $\rho = \sum_a \rho_a$.

A single particle is located at one of the lattice sites at integer times $t = 0, 1, 2,...$ and moves with a constant velocity $\mathbf{c}_i$ ($i = 0, 1,..., b - 1$) until it hits a scatterer. The set of allowed velocities $\{\mathbf{c}_i\}$ consists of b nearest neighbor lattice vectors. The above types of models are generally referred to as Lorentz gases. If the moving particle hits a scatterer of type a with incoming velocity $\mathbf{c}_j$, its outgoing velocity will be $\mathbf{c}_i$ with probability $W_{aij} = \delta_{ij} + T_{aij}$, normalized as $\sum_i T_{aij} = 0$. The moving particle is described by the occupation number $n_i(\mathbf{r}, t)$, which equals 1 if velocity channel $\mathbf{c}_i$ at site $\mathbf{r}$ is occupied at (precollision) time t and vanishes otherwise.

On long time scales the average motion of the moving particle is diffusive. The diffusion coefficient is in general a tensorial property $D_{\alpha\beta}$ with $\alpha, \beta = \{x, y, z,..., d\}$, which may have nonvanishing off-diagonal elements. It is defined through the Green–Kubo relation,

$$D_{\alpha\beta} = \frac{1}{2} \left[\sum_{t=0}^{\infty} (\langle v_\alpha(t) \, v_\beta(0) \rangle_0 + \langle v_\beta(t) \, v_\alpha(0) \rangle_0) - \frac{1}{d} \delta_{\alpha\beta} \right]$$

$$= \frac{1}{2} \left(\langle c_\alpha | \, \Gamma \, | c_\beta \rangle + \langle c_\beta | \, \Gamma \, | c_\alpha \rangle - \frac{1}{d} \delta_{\alpha\beta} \right) \tag{2.1}$$

Here $v_\alpha(t) = \sum_{ri} c_{i\alpha} n_i(\mathbf{r}, t)$ is the velocity of the moving particle. On the second line of (2.1) the time correlation function has been expressed in terms of the kinetic propagator, which is the most fundamental quantity for describing nonequilibrium properties. The average $\langle \cdots \rangle_0$ involves an average over the stationary distribution of the moving particle in a fixed configuration of scatterers and a subsequent average over all configurations $\mathbf{s}$ of scatterers. If the average only refers to the configurations $\mathbf{s}$ of the scatterers, we write $\langle \cdots \rangle$. The $b \times b$ matrix Γ is defined as

$$\Gamma = \sum_{t=0}^{\infty} \sum_r G(\mathbf{r}, t) \tag{2.2}$$

where $G_{ij}(\mathbf{r}, t)$ is the kinetic propagator

$$G_{ij}(\mathbf{r}, t) = bV \langle n_i(\mathbf{r}, t)\, n_j(\mathbf{0}, 0)\, \psi_j(\mathbf{0}) \rangle / \langle \psi \rangle \simeq bV \langle n_i(\mathbf{r}, t)\, n_j(\mathbf{0}, 0) \rangle \qquad (2.3)$$

The overlap function $\psi_i(\mathbf{r}\,|\,\mathbf{s})$ equals 1 or 0 when the state $\{\mathbf{r}, \mathbf{c}_i\}$ is physically accessible or inaccessible, respectively, so that $\langle \psi \rangle$ is the free volume fraction. In the case of point scatterers, $\psi_i(\mathbf{r}\,|\,\mathbf{s}) = 1$ for all the states $\{\mathbf{r}, \mathbf{c}_i\}$. At $t = 0$, $G_{ij}(\mathbf{r}, 0) = \delta_{ij}\delta(\mathbf{r}, \mathbf{0})$, where $\delta(\mathbf{r}, \mathbf{0})$ is a d-dimensional Kronecker delta function. In the present paper we concentrate on the low-density limit and discard all terms that contribute only to higher-order density corrections. This implies, for instance, that the overlap function ψ_i is set equal to unity.

It is convenient to consider G as a $b \times b$ matrix and the Cartesian component c_α with $\alpha = \{x, y,..., d\}$ itself as a b-vector in state space with components $\{c_{ja};\ j = 0, 1,..., b-1\}$. We further introduce a scalar product of b-vectors $u(c)$ and $v(c)$ as

$$\langle u\,|\,v \rangle = \frac{1}{b} \sum_{j=0}^{b-1} u^*(c_j)\, v(c_j) \qquad (2.4)$$

where the asterisk denotes complex conjugation.

In order to develop the kinetic theory for Lorentz gases, the equation of motion for the microscopic variables must be constructed. The time evolution of the moving particle consists of two steps, a collision step, described by the collision operator $I(\mathbf{r}\,|\,\mathbf{s})$, and a propagation step, described by the streaming operator $\mathscr{S}$. The equation for the (backward) time evolution for the occupation numbers $n_i(\mathbf{r}, t)$ has been derived in ref. 7. It has the standard form of the microdynamic equation in lattice gas automata (LGA), i.e.,

$$n_i(\mathbf{r}, -t-1) = \mathscr{S} n_i(\mathbf{r}, -t) + \sum_j I_{ij}(\mathbf{r}\,|\,\mathbf{s})\, \mathscr{S} n_j(\mathbf{r}, -t) \qquad (2.5)$$

where t is nonnegative ($t \geqslant 0$). The streaming operator $\mathscr{S}$, defined as

$$\mathscr{S} n_i(\mathbf{r}, t) \equiv n_i(\mathbf{r} + \mathbf{c}_i, t) \qquad (2.6)$$

describes the propagation step. In the low-density limit relevant for this paper the collision operator $I(\mathbf{r}\,|\,\mathbf{s})$ contains only binary collisions. In Lorentz models with·a *mixture of different point* scatterers the collision operator has the form

$$I_{ij}(\mathbf{r}\,|\,\mathbf{s}) = \sum_a s_a(\mathbf{r})\, T_{aij} \qquad (2.7)$$

where a labels the different species. Two examples are given in Fig. 1, the details of which are described in Appendix A. In Lorentz models with *extended* scatterers the collision operator at low density of scatterers can be written as

$$I_{ij}(\mathbf{r}\,|\,\mathbf{s}) = \sum_a s(\mathbf{r}+\mathbf{c}_{i+a})\, T_{aij} \qquad (2.8)$$

where a labels the different impact parameters. Four different models with extended scatterers are introduced in Fig. 2. The models with extended scatterers are variations on the hexagon models of ref. 6, and the explicit form of the T-matrices is given in Appendix B. In case of the triangle model, Eq. (2.8) is slightly modified [see (B.7)], because a scatterer is assigned to the center of a unit cell, and not to the lattice site.

For illustrational purposes we give the explicit form of the T-matrix for a square lattice model with identical point scatterers. If the moving particle hits a scatterer, it is transmitted with probability α, reflected with probability β, and deflected in either of the two perpendicular directions with probability γ, where $\alpha + \beta + 2\gamma = 1$. In this case the collision operator T_{ij} is a 4×4 matrix of the form

$$T = (\alpha - 1)\mathbf{1} + \beta \mathcal{D}^2 + \gamma(\mathcal{D} + \mathcal{D}^3) \qquad (2.9)$$

where the rotation matrix $\mathcal{D}$ acts on a velocity label i as

$$(\mathcal{D}^n u)_i \equiv \sum_j (\mathcal{D}^n)_{ij}\, u_j = u_{i+n} \qquad (n = 1, 2,...) \qquad (2.10)$$
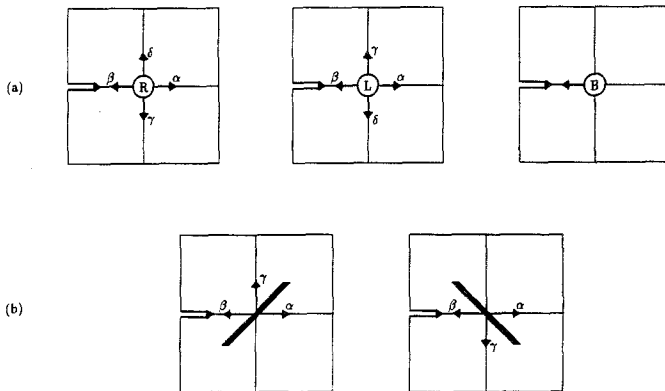

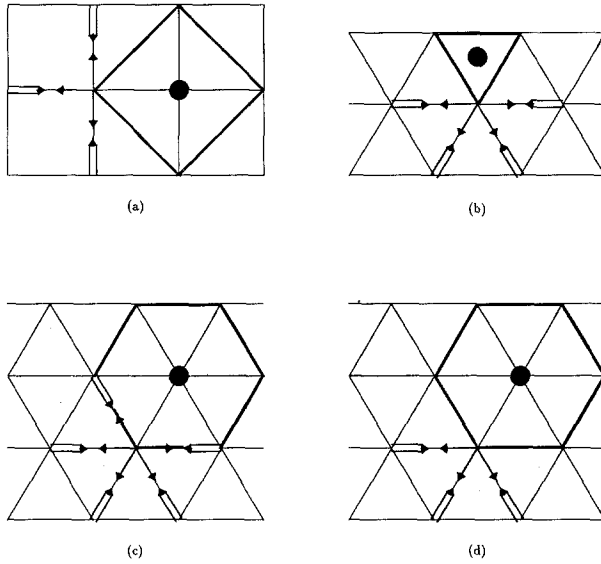Fig. 1. Mixed point scatterer models: (a) rotators and (b) mirrors.

Fig. 2. Extended scatterer models: (a) diamonds, (b) triangles, (c) hexagons A, and (d) hexagons B.

In a more compact notation, the evolution equation (2.5) can be written in the equivalent form

$$n(-t) = [(\mathbf{1} + \mathcal{I}(\mathbf{s}))\mathcal{S}]^t \, n(0) \tag{2.11}$$

where the occupation numbers $\{n_i(\mathbf{r})\}$ have been considered as a vector n with bV components, $(n)_{ri} = n_i(\mathbf{r})$, and the operators $\mathcal{S}$ and $\mathcal{I}$ acting on n have been represented as $bV \times bV$ matrices with matrix elements

$$\mathcal{S}_{ri,r'j} = \delta_{ij}\delta(\mathbf{r}', \mathbf{r} + \mathbf{c}_i)$$
$$\mathcal{I}_{ri,r'j}(\mathbf{s}) = I_{ij}(\mathbf{r}\,|\,\mathbf{s})\,\delta(\mathbf{r}, \mathbf{r}') \tag{2.12}$$

Similarly, the kinetic propagator (2.3) can be written in the compact notation

$$G_{ij}(\mathbf{r}, t) = \left\langle \left\{ [(\mathbf{1} + \mathcal{I}(\mathbf{s}))\mathcal{S}]^t \right\}_{0j,ri} \right\rangle \tag{2.13}$$

3. REPEATED RING APPROXIMATION

Before developing the repeated ring approximation, it is instructive to consider the mean field or Boltzmann approximation in the low-density

limit, where possible excluded volume effects and multiple collisions can be neglected. The Boltzmann approximation only accounts for uncorrelated collision sequences in which the moving particle never returns to a scatterer visited before. Therefore each collision operator $\mathscr{I}(\mathbf{s})$ in (2.13) can be replaced by its average,

$$\langle \mathscr{I}(\mathbf{s}) \rangle_{ri, r'j} = \langle I_{ij}(\mathbf{r} \mid \mathbf{s}) \rangle \, \delta(\mathbf{r}, \mathbf{r}') \equiv -\Lambda^0_{ij} \delta(\mathbf{r}, \mathbf{r}') \tag{3.1}$$

which is translationally invariant and Λ^0_{ij} is a $b \times b$ matrix given by

$$\Lambda^0_{ij} = -\sum_a \rho_a T_{aij} \quad \text{(point)}$$

$$= -\sum_a \rho T_{aij} \quad \text{(extended)} \tag{3.2}$$

In the Boltzmann approximation the propagator Γ in (2.2) is $\Gamma^0 = 1/\Lambda^0$ and the diffusion coefficient (2.1) becomes

$$D^0_{\alpha\beta} = \frac{1}{2} \left(\langle c_\alpha | \frac{1}{\Lambda^0} | c_\beta \rangle + \langle c_\beta | \frac{1}{\Lambda^0} | c_\alpha \rangle - \frac{1}{d} \delta_{\alpha\beta} \right) \tag{3.3}$$

Next we turn to the repeated ring approximation. Based on the motivation given in the introduction, we restrict ourselves to low densities of scatterers $(\rho \to 0)$ and we only account for the simplest correlated collision sequences, the so-called ring collisions, in which the moving particle returns repeatedly to the same scatterer. This can be done using standard resummation methods of kinetic theory.[8] We start with a mixture of point scatterers, as occurring in the models of Appendix A. In the repeated ring summation the fluctuating operator $\mathscr{I}(\mathbf{s})$ in (2.13) is replaced by a nonfluctuating or effective one, similar to (3.1) with Λ^0 replaced by Λ. The Fourier transform of the kinetic propagator (2.13) takes the form

$$\hat{\Gamma}(\mathbf{q}) = \sum_{t=0}^{\infty} \sum_r \left[\exp(-\hat{\imath} \mathbf{q} \cdot \mathbf{r}) \right] G(\mathbf{r}, t)$$

$$= \left[\exp(-\hat{\imath} \mathbf{q} \cdot \mathbf{c}) \right] \left[\exp(-\hat{\imath} \mathbf{q} \cdot \mathbf{c}) - \mathbf{1} + \Lambda \right]^{-1} \tag{3.4}$$

where $\hat{\imath} = (-1)^{1/2}$ and $[\exp(\hat{\imath} \mathbf{q} \cdot \mathbf{c})]_{ij} = \delta_{ij} \exp(\hat{\imath} \mathbf{q} \cdot \mathbf{c}_i)$. The collision operator Λ sums the repeated ring collisions, i.e.,

$$\Lambda = -\sum_a \rho_a \{ T_a + T_a R T_a + T_a R T_a R T_a + \cdots \}$$

$$= -\sum_a \frac{\rho_a T_a}{1 - R T_a} \tag{3.5}$$

where the ring operator is defined with the help of (3.4) as

$$R = \frac{1}{V} \sum_{\mathbf{q} \in \mathrm{1BZ}} [\exp(i\mathbf{q} \cdot \mathbf{c})] \, \hat{\mathit{\Gamma}}(\mathbf{q}) = \int_q [\exp(-i\mathbf{q} \cdot \mathbf{c}) - \mathbf{1} + \mathit{\Lambda}]^{-1} \quad (3.6)$$

The element R_{ij} represents the total return probability with arrival velocity $\mathbf{c}_i$ to a site visited before, when its departure velocity was $\mathbf{c}_j$. The $\mathbf{q}$-sum extends over the first Brillouin zone of the reciprocal d-dimensional lattice $\mathscr{L}^*$ corresponding to the direct lattice $\mathscr{L}$ under consideration. The wave vector $\mathbf{q} = \sum_s q_s \mathbf{e}_s^*$ ($s = 1, 2,..., d$) is a reciprocal lattice vector and $\{\mathbf{e}_s^*\}$ is the set of independent reciprocal basis vectors. As we have imposed periodic boundary conditions on the macroscopic system with $V = L^d$ sites, the components q_s are given by $q_s = 2\pi v_s / L$ with $v_s = -\frac{1}{2}L + 1,..., -1, 0, 1, 2,..., \frac{1}{2}L$. The integration symbol in (3.6) is defined as

$$\int_q \cdots = \frac{1}{V} \sum_{\mathbf{q} \in \mathrm{1BZ}} \cdots \xrightarrow{V \to \infty} \prod_{s=1}^{d} \left(\int_{-\pi}^{\pi} \frac{dq_s}{2\pi} \right) \cdots \quad (3.7)$$

In the thermodynamic limit ($V \to \infty$) the summation over the first Brillouin zone can be replaced by an integration. For general lattices ($q_1, q_2,...$) are non-Cartesian components of $\mathbf{q}$. For instance, for the infinitesimal volume element on the triangular lattice, $dq_1 \, dq_2 = \frac{1}{2}\sqrt{3} \, dq_x \, dq_y$, where q_α ($\alpha = x, y$) are Cartesian components. The first term in the collision operator (3.5) is the Boltzmann collision operator; the next term, $T_a R T_a$, accounts for the first return to the same scatterer, labeled a; etc.

The combined equations (3.5) and (3.6), containing the unknown matrices $\mathit{\Lambda}$ and R, constitute a *self-consistent* set of equations, from which $\mathit{\Lambda}$ and R can be determined for mixtures of point scatterers. Once $\mathit{\Lambda}$ is determined, the transport coefficients can be calculated for any density using (2.1) and (3.4) with $\mathit{\Gamma} = \hat{\mathit{\Gamma}}(\mathbf{q} = \mathbf{0})$. In general, such calculations have to be performed numerically. However, in the limit of a low concentration of scatterers the system of equations (3.5) and (3.6) simplifies sufficiently to allow an analytic solution, as will be shown below.

Consider next the repeated ring approximation for models with finite-size scatterers. The collision operator is given by (2.8). The label a runs over all possible impact parameters of the moving particle in a (binary) collision with a single scatterer. Therefore the repeated ring approximation for extended scatterers reduces for $\rho \to 0$ to a simple matrix relation,

$$\mathit{\Lambda} = -\sum_a \frac{\rho T_a}{\mathbf{1} - R T_a} \quad (3.8)$$

where the sum is restricted to binary collisions, a denotes the different impact parameters, and ρ is the density of scatterers. The diffusion coef-

ficient $D_{\alpha\beta}$ (α, $\beta = x$, y) in the repeated ring approximation is given by (3.3) with Λ^0 replaced by Λ.

The most convenient way to evaluate D is to study the matrix Λ in (3.5) or (3.8) and to determine its eigenvectors and eigenvalues. Not only the symmetry properties of Λ, but also those of the matrices R and T_a are determined by the symmetries of the scatterers and of the underlying lattice, as explained in Appendix C. Symmetry considerations immediately yield the complete set of common eigenvectors φ_l ($l = 0, 1,..., b-1$) of the set of commuting matrices with the appropriate lattice symmetries.

By convention, we denote the eigenvalues and eigenvectors as

$$M \,|\varphi_l\rangle = m_l \,|\varphi_l\rangle \qquad (l = 0, 1,..., b-1) \tag{3.9}$$

where $\langle \varphi_l | \varphi_{l'} \rangle = \delta_{ll'}$. The b-vectors $|\varphi_l\rangle$ for different symmetries and corresponding eigenvalues are explicitly given in Appendix C. For the eigenvalues we use the notation

$$M = \{R, \Lambda, W_a, T_a,...\}$$
$$m_l = \{r_l, \lambda_l, w_{al}, -\tau_{al},...\} \tag{3.10}$$

In case the scatterers have only *rotation symmetry*, but not reflection symmetry (see Appendix A; rotator model), the relevant eigenfunctions are $|\varphi_1\rangle = |c_x + \hat{\imath}c_y\rangle$ and $|\varphi_{b-1}\rangle = |\varphi_1^*\rangle = |c_x - \hat{\imath}c_y\rangle$ with corresponding eigenvalues λ_1 and $\lambda_{b-1} = \lambda_1^*$. The diffusion tensor for the square and triangular lattices is diagonal, i.e.,

$$D_{\alpha\beta} = \delta_{\alpha\beta} \operatorname{Re}(2\lambda_1)^{-1} \tag{3.11}$$

where Re denotes the real part. In case the scatterers have only *reflection symmetry* (see Appendix A; mirror model), the relevant eigenfunctions for the square lattice are $|\varphi_1\rangle = |c_x + c_y\rangle$ and $|\varphi_3\rangle = |c_x - c_y\rangle$ with eigenvalues λ_1 and λ_3, respectively. The diffusion tensor is

$$D_{xx} = D_{yy} = \frac{1}{4}\left(\frac{1}{\lambda_1} + \frac{1}{\lambda_3}\right)$$
$$D_{xy} = D_{yx} = \frac{1}{4}\left(\frac{1}{\lambda_1} - \frac{1}{\lambda_3}\right) \tag{3.12}$$

In case the system has on average both rotation and reflection symmetries, $\lambda_1 = \lambda_3$ and the diffusion tensor is again diagonal. The above expressions hold also for the Boltzmann approximation with λ_l replaced by λ_l^0.

4. RING INTEGRAL AT LOW DENSITY

In this section the eigenvalues r_l of the ring integral R, defined in (3.6), are evaluated for small concentration of scatterers ($\rho \to 0$), starting from the expression

$$r_l = \int_q \langle \varphi_l | \frac{1}{\exp(-i\mathbf{q}\cdot\mathbf{c}) - \mathbf{1} + \Lambda} | \varphi_l \rangle \qquad (4.1)$$

Analytic evaluation of this d-dimensional q-integration over elements of an inverse $b \times b$ matrix is not possible in general, although in two very special cases of a square lattice model[2, 9] the integral has been evaluated analytically for general density.

In the low-density limit ($\rho \to 0$), however, the integration in (4.1) can be carried out analytically and yields a nontrivial result. First, suppose that one takes the limit $\rho \to 0$ of (4.1) by interchanging q-integration and ρ-limit. As all matrix elements of Λ are of $\mathcal{O}(\rho)$ on account of (3.6) and (3.8), one finds the simple result

$$\int_q [\exp(-i\mathbf{q}\cdot\mathbf{c}) - \mathbf{1}]^{-1} = -\tfrac{1}{2} \qquad (4.2)$$

However, the limits $\rho \to 0$ and $\mathbf{q} \to 0$ cannot be interchanged, and the integration region at small $\mathbf{q}$ has to be investigated separately. Therefore we consider the difference between R in (3.6) and the naive limit (4.2), i.e.,

$$\int_q \Delta(\mathbf{q}) = \int_q \{ [\exp(-i\mathbf{q}\cdot\mathbf{c}) - \mathbf{1} + \Lambda]^{-1} - [\exp(-i\mathbf{q}\cdot\mathbf{c}) - \mathbf{1}]^{-1} \}$$

$$= - \int_q [\exp(-i\mathbf{q}\cdot\mathbf{c}) - \mathbf{1} + \Lambda]^{-1} \Lambda [\exp(-i\mathbf{q}\cdot\mathbf{c}) - \mathbf{1}]^{-1} \qquad (4.3)$$

and we consider a small sphere around the origin with a radius $|\mathbf{q}|$ proportional to ρ. As $\Lambda \sim \mathcal{O}(\rho)$, simple scaling arguments show that the contribution of this region to the integral (4.3) is of $\mathcal{O}(\rho^{d-1})$. In all dimensions except $d = 1$ this contribution can be neglected with respect to (4.2).

Next, we consider a one-dimensional strip $\mathscr{A}_k$ on a 2D lattice (and, more generally, a $(d-1)$-dimensional slab in a d-dimensional lattice), perpendicular to $\mathbf{c}_k$ and $\mathbf{c}_{k+b/2}$, where $q_k = \mathbf{q}\cdot\mathbf{c}_k$ ($k = 0, 1,..., b/2 - 1$) is small of $\mathcal{O}(\rho)$ and where the remaining q-components extend over the total interval $(-\pi, \pi)$. The contribution of strip $\mathscr{A}_k$ to the integral (4.3) can be estimated by rescaling only the component $q_k = \rho \bar{q}_k$. It gives a singular contribution of $\mathcal{O}(\rho^0)$, which is of the same order of magnitude as (4.2).

Therefore, we need the dominant behavior of $\Delta(\mathbf{q})$ in strips $\mathscr{A}_k$,

obtained by letting $q_k = \mathbf{q} \cdot \mathbf{c}_k$ approach to zero. For that purpose, we write the matrix $\varDelta(\mathbf{q})$ in (4.3) as

$$\varDelta(\mathbf{q}) = \sum_{n=1}^{\infty} (-G\varLambda)^n G$$

$$G = [\exp(-\hat{\imath}\mathbf{q} \cdot \mathbf{c}) - \mathbf{1}]^{-1} = -\tfrac{1}{2} + \tfrac{1}{2} \sum_{k=0}^{b/2-1} [\sin q_k/(1 - \cos q_k)] \hat{\imath} V_k$$

$$\tag{4.4}$$

Here the diagonal matrix $G_{ij} = \delta_{ij}(\exp(-\hat{\imath}q_j - 1)^{-1}$ has been expressed in terms of the b-dimensional diagonal matrices

$$(V_k)_{ij} = \delta_{ij}(\delta_{jk} - \delta_{j,k+b/2}) \tag{4.5}$$

They have the property

$$V_k^n V_l^m = \delta_{kl} V_k^{n+m} = \delta_{kl} \begin{cases} V_k & \text{if} \quad n+m = \text{odd} \\ V_k^2 & \text{if} \quad n+m = \text{even} \end{cases} \tag{4.6}$$

To summarize the results of this section so far, we have for the eigenvalues of the ring operator,

$$r_l = -\tfrac{1}{2} + \sum_{k=0}^{b/2-1} \int_{\mathscr{A}_k} \langle \varphi_l | \varDelta | \varphi_l \rangle \tag{4.7}$$

with $\varDelta$ given by (4.3) and (4.4). The integration in the kth term extends over the strip $\mathscr{A}_k$ with $q_k \sim \mathcal{O}(\rho)$, where G in (4.4) is given by

$$G \simeq (\hat{\imath}/q_k) V_k + \mathcal{O}(q_k^0) \tag{4.8}$$

The most important property for our analysis, which applies to strip $\mathscr{A}_k$ only, is

$$(G\varLambda)^2 |V_k\rangle = (-\mu_+ \mu_-/q_k^2) |V_k\rangle$$

$$(G\varLambda)^2 |V_k^2\rangle = (-\mu_+ \mu_-/q_k^2) |V_k^2\rangle$$

$$\tag{4.9}$$

Here the b-vectors are $|V_k^n\rangle =^d V_k^n |1\rangle$ with $|1\rangle = (1, 1,..., 1)$, and μ_+ and μ_- represent the average of the even $(+)$ or odd $(-)$ eigenvalues of $\varLambda$, with

$$\mu_+ = \frac{2}{b} \sum_l^{(+)} \lambda_l$$

$$\mu_- = \frac{2}{b} \sum_l^{(-)} \lambda_l$$

$$\tag{4.10}$$

where the superscripts denote a summation over even ($+$) or odd ($-$) l values only. To prove (4.9), we decompose the b-vectors $|V_k\rangle$ or $|V_k^2\rangle$ into eigenvectors $|\varphi_l\rangle$ of Λ (see Appendix C). Subsequent application of $G\Lambda$ yields respectively $|V_k^2\rangle$ or $|V_k\rangle$ on account of (4.6). Consequently, the matrix $(G\Lambda)^2$ in strip $\mathscr{A}_k$ has $|V_k\rangle$ and $|V_k^2\rangle$ as eigenvectors.

We illustrate this result for a square lattice model ($b=4$) with rotationally symmetric scatterers and eigenfunctions $|\varphi_l\rangle$ given by (C.4). Consider strip $\mathscr{A}_0$, where

$$GA \, |V_0\rangle = \frac{1}{2} G(\lambda_1 \, |\varphi_1\rangle + \lambda_3 \, |\varphi_3\rangle) = \frac{\hat{\imath}}{q_0} \mu_- \, |V_0^2\rangle$$

$$GA \, |V_0^2\rangle = \frac{1}{2} G(\lambda_0 \, |\varphi_0\rangle + \lambda_2 \, |\varphi_2\rangle) = \frac{\hat{\imath}}{q_0} \mu_+ \, |V_0\rangle \tag{4.11}$$

In the left equalities, (C.4) has been used together with (3.9) and (3.10); in the right equalities, (C.3) was used together with (4.6). If one deletes in (4.11) the intermediate equality, referring to the square lattice, one obtains the basic relations, which hold for all lattices, all types of scatterers, and all allowed orientations of the strip $\mathscr{A}_k$ ($k = 0, 1,..., b/2 - 1$). Application of $G\Lambda$ to both equations in (4.11) finally yields (4.9).

The derivation of this result for other strips $\mathscr{A}_k$, for scatterers with different symmetries (e.g., reflection), and for different lattices and dimensionalities is completely analogous and can be carried out straightforwardly using the relations of Appendix C. Repeated application of (4.9) yields $\Lambda(\mathbf{q})$ in the strip $\mathscr{A}_k$ for all lattices and all symmetries of scatterers. The contribution of this strip to the integral in (4.3) becomes then

$$\int_{\mathscr{A}_k} \langle V_k| \, \Lambda \, |V_k\rangle = \frac{2}{b} \int_{\mathscr{A}_k} \frac{\mu_+}{q_k^2 + \mu_+ \mu_-} = \frac{1}{b} \left(\frac{\mu_+}{\mu_-} \right)^{1/2}$$

$$\int_{\mathscr{A}_k} \langle V_k^2| \, \Lambda \, |V_k^2\rangle = \frac{2}{b} \int_{\mathscr{A}_k} \frac{\mu_-}{q_k^2 + \mu_+ \mu_-} = \frac{1}{b} \left(\frac{\mu_-}{\mu_+} \right)^{1/2} \tag{4.12}$$

where the relation $\langle V_k| V_k \rangle = 2/b$ has been used [see (2.4) and (C.3)]. The contribution of every strip $\mathscr{A}_k$ ($k = 0, 1,..., b/2 - 1$) is identical. A direct application of (4.12) to the *ring eigenvalue* (4.7) yields in the *low-density limit*

$$r_l = \begin{cases} r_0 = r_2 = \cdots = -\dfrac{1}{2} + \dfrac{1}{2} \left(\dfrac{\mu_-}{\mu_+} \right)^{1/2} & (l = 0, 2, 4,...) \\[4mm] r_1 = r_3 = \cdots = -\dfrac{1}{2} + \dfrac{1}{2} \left(\dfrac{\mu_+}{\mu_-} \right)^{1/2} & (l = 1, 3, 5,...) \end{cases} \tag{4.13}$$

where the formulas (C.4), (C.6), and (C.8), which express $|\varphi_l\rangle$ in terms of $|V_k\rangle$ or $|V_k^2\rangle$, have been used. These results agree with the only available result for r_l, which has been obtained for a square lattice model with scatterers having rotational symmetry.[2, 9]

As a result of (4.13), the self-consistent set of transcendental equations (3.5), or (3.8), and (3.6) for the unknown matrices Λ and R has been reduced in the low-density limit to a set of algebraic equations for the unknown eigenvalues λ_l and r_l, which will be cast into an equation for a single variable. We start with point scatterers of different types, where the eigenvalues λ_l of the ring collision operator (3.5) are

$$\lambda_l = \sum_a \frac{\rho_a \tau_{al}}{1 + r_l \tau_{al}} \tag{4.14}$$

where τ_{al} are the known eigenvalues of $-T_a$ and where r_l is given in terms of λ_k through (4.13). A convenient change of variables in (4.13) is $y = (\mu_-/\mu_+)^{1/2}$. Substitution of (4.13) into (4.14) then gives

$$\lambda_l = \begin{cases} \displaystyle\sum_a \frac{2\rho_a}{y + \eta_{al}} & (l = \text{even}) \\[3mm] \displaystyle\sum_a \frac{2\rho_a y}{1 + \eta_{al} y} & (l = \text{odd}) \end{cases} \tag{4.15}$$

and we have introduced

$$\eta_{al} = \frac{2}{\tau_{al}} - 1 \tag{4.16}$$

Combination of (4.15) with $y^2 \sum_l^{(+)} \lambda_l = \sum_l^{(-)} \lambda_l$ yields, after some rearrangements, an algebraic equation for y, i.e.,

$$\sum_a \rho_a \left\{ \sum_{l \neq 0}^{(+)} \frac{y}{y + \eta_{al}} - \sum_l^{(-)} \frac{1}{1 + \eta_{al} y} \right\} = 0 \tag{4.17}$$

Comparison of (3.8) and (3.5) shows that the only modification for a set of *identical scatterers of finite size* is that ρ_a in (4.15) and (4.17) is replaced by ρ. The summation over a refers here to different values of the impact parameter, where the corresponding scattering operator is described by T_a (see Appendix B).

Equations (4.15) and (4.17) are the most important results of this paper. From their solution one can calculate the approximate eigenvalues λ_l of the repeated ring collision operator Λ, which determine directly the diffusion coefficient at a low concentration of scatterers through (3.3) with Λ^0 replaced by Λ.

5. IDENTICAL POINT SCATTERERS

The solution of the self-consistent repeated ring approximation (4.15)–(4.17) can also be applied to a Lorentz gas with identical point scatterers that backscatter. For such models the diffusion coefficient for a small concentration of scatterers ($\rho \to 0$) was recently calculated in ref. 5 by an exact enumeration of all possible trajectories on a Cayley tree. Here we will show that the repeated ring approximation—which only sums a small subset of all contributing trajectories—does give the exact result for $\rho \to 0$ if all scatterers are *identical* and *point like*.

To begin, we quote the result of ref. 5 for the kinetic propagator (2.2) as $\rho \to 0$,

$$\Gamma = \frac{1}{\rho}\left(-\frac{1}{T} + \frac{X}{1-X}\right) \tag{5.1}$$

where $W_{ij} = \delta_{ij} + T_{ij}$ is the matrix of transition probabilities and X_{ij} the matrix of first return probabilities to the initial interval. On a Cayley tree X_{ij} is only nonvanishing for $c_j = -c_i$ or $i = j + b/2$. The eigenvectors $|\varphi_l\rangle$ ($l = 0, 1,..., b-1$) of W and X are determined by the lattice symmetries and are given in Appendix C. The corresponding eigenvalues are $w_l = 1 - \tau_l$ and $x_l = (-1)^l x$, where the first return probability x satisfies the polynomial equation

$$\frac{b}{1-x^2} = \frac{1}{1-x} + \overset{(+)}{\underset{l \neq 0}{\sum}} \frac{1}{1-xw_l} + \overset{(-)}{\underset{l}{\sum}} \frac{1}{1+xw_l} \tag{5.2}$$

On the other hand, for a regular lattice of point scatterers of the same type and for low concentration of scatterers, the repeated ring propagator (3.4) combined with (3.5) can be cast into the form

$$\hat{\Gamma}(0) = \frac{1}{\Lambda} = \frac{1}{\rho}\left(-\frac{1}{T} + R\right) \tag{5.3}$$

The eigenvalues r_l of R are given by (4.13) with $y \equiv (\mu_-/\mu_+)^{1/2}$ satisfying (4.17). That equation becomes now

$$\overset{(+)}{\underset{l \neq 0}{\sum}} y\bigg/\left[y + \frac{1+w_l}{1-w_l}\right] - \overset{(-)}{\underset{l}{\sum}} 1\bigg/\left[1 + \frac{1+w_l}{1-w_l}y\right] = 0 \tag{5.4}$$

where (4.16) and $w_l = 1 - \tau_l$ have been used. Comparison of the right-hand sides of (5.1) and (5.3) suggests the identification $R \rightleftharpoons X/(1-X)$. This implies that the eigenvalue $r_1 = -\frac{1}{2} + \frac{1}{2}y$ in (4.13) equals $-x/(1+x)$, or

$$y = \frac{1+x}{1-x} \tag{5.5}$$

Indeed, substitution of (5.5) into (5.4) yields, after some rearrangements, an equation for x that is identical to the exact equation (5.2) obtained in ref. 5 from the exact enumeration method. Therefore, the results obtained in Section 4 turn out to be exact in the limit of vanishing concentration of point scatterers of the same type.

6. COMPARISON WITH SIMULATIONS

6.1. Identical Point Scatterer

In this section exact and approximate results obtained from kinetic theory will be compared with computer simulations for various models of point and extended scatterers. However, there is a complication because the analytic results from ring kinetic theory only apply to the limiting case of low density ($\rho \to 0$), whereas simulations need to be performed at finite densities.

We consider first a lattice gas with *identical* stochastic *point scatterers*, as defined in (2.9). At low densities ($\rho \to 0$) the kinetic propagator Γ is given by the exact expression (5.1). For a completely filled lattice ($\rho = 1$) the lattice gas reduces to a random walk, where the exact propagator is given by $\Gamma = -(\rho T)^{-1} - \frac{1}{2}$. In ref. 5 a probabilistic argument was given to include a density-dependent correction in (5.1), reading

$$\Gamma = -\frac{\bar{l}}{T} + \frac{(\bar{l}-1)X}{1-X} \tag{6.1}$$

where $\bar{l} = 1/\rho$ is the mean free path. The formula linearly interpolates between two exact limiting cases for $\rho \to 0$ and $\rho \to 1$. It predicts for the diffusion coefficient

$$D = D_{xx} = \frac{1}{2}\left\{\frac{\bar{l}}{\tau_1} - \frac{(\bar{l}-1)x}{1+x} - \frac{1}{2}\right\} \tag{6.2}$$

where we have used (2.1) and eigenvalues (τ_1, x), defined through $Tc_x = -\tau_1 c_x$ and $Xc_x = -xc_x$ with $\tau_1 = 1 - \alpha + \beta$, as can be obtained from (2.9), (C.1), and (C.3). To compare theory and simulations, we can use the result (6.2) for the diffusion coefficient at finite densities, which extrapolates to the $\rho \to 0$ result, as predicted by the present theory. This is illustrated in Fig. 3 by the solid curve and simulation data (squares) with parameters in (6.2) set at $\alpha = \beta = 1/3$ and $\gamma = 1/6$.

The plot also illustrates that the Boltzmann approximation (dashed line) gives a very poor prediction of the diffusion coefficient at low densities.

In ref. 2 simulation results for the same model have been compared with the effective medium approximation. This approximation has a very complex structure, which, for finite densities, can only be analyzed numerically.

6.2. Mixed Point Scatterers

For models with mixed scatterers, as introduced in Fig. 1 of Section 2, no analytic results for the diffusion coefficient are available for *finite* densities. Simulation results (triangles) for the two-component mirror model, as defined in Fig. 1b, are also shown in Fig. 3. The parameters for this model, as defined in (A.2) of Appendix A, are $\alpha = \beta = \gamma = 1/3$ with normalization $\alpha + \beta + \gamma = 1$. There are equal concentrations of R-mirrors and L-mirrors ($\rho_R = \rho_L = \frac{1}{2}\rho$) and no B-scatterers ($\rho_B = 0$). Note the difference in normalization of the rates α, β, and γ from those described in (2.9). The diffusion coefficients at densities above $\rho = 0.01$ were obtained by measuring the mean square displacement of a particle that moves on a lattice within a fixed array of scatterers. The result at the extremely low density $\rho = 0.01$ was obtained on a Cayley tree that corresponds to this particular model.

According to the repeated ring approximation, the diffusion coefficient as $\rho \to 0$ for the mirror model is given by (3.12) with λ_l in (4.15). If we restrict ourselves to equal concentrations of right and left mirrors, i.e.,
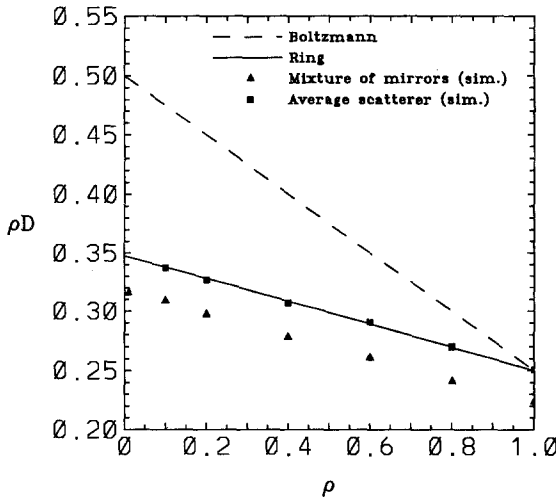

Fig. 3. Comparison of simulations and theory for the diffusion coefficient $D(\rho)$.

$\rho_R = \rho_L = C\rho$ and $\rho_B = C_B \rho$, the eigenvalues in (3.12) are equal and given by

$$\lambda_1 = \lambda_3 = 2\rho y \left\{ \frac{C}{1+\eta_{R1} y} + \frac{C}{1+\eta_{R3} y} + C_B \right\} \tag{6.3}$$

The quantity y is the positive root of (4.17), which reads for the present case

$$\frac{y}{y+\eta_{R2}} - \frac{1}{1+\eta_{R1} y} - \frac{1}{1+\eta_{R3} y} = \frac{C_B}{C} \tag{6.4}$$

where η_{al} follows from (4.16) and (A.5) as

$$\eta_{R1} = (1-\beta)/\beta, \qquad \eta_{R2} = (1-\gamma)/\gamma, \qquad \eta_{R3} = \alpha/(1-\alpha) \tag{6.5}$$

For the parameter values used in the simulations, the solution of (6.4) is $y = 1 + \sqrt{3}$ and the diffusion coefficient $D = (2\lambda_1)^{-1}$ for $\rho \to 0$ becomes $\rho D = \frac{1}{4}(3 - \sqrt{3}) \simeq 0.317$. Figure 3 and Table I show that this limiting value is in very good agreement with the simulation results (triangles).

The Boltzmann approximation $D^0 = (2\lambda_1^0)^{-1}$ for $\rho \to 0$ can be obtained from (6.3) by setting $y = 1$ and using (4.16) and (A.5) with the formula $\lambda_1^0 = 2\rho\{C(1-\alpha+\beta) + C_B\}$. For the parameters used in the simulations ($\alpha = \beta = 1/3$, $C = 1/2$, $C_B = 0$) this gives in the low-density limit $\rho D^0 = 1/2$ (see Fig. 3 and Table I), which is a very poor estimate of the diffusion coefficient.

A crude estimate of the diffusion coefficient for *all* densities may be obtained from the *average scatterer* approximation. In this approximation the different types of scatterers in the mixture are replaced by a single

Table I. Values for $\rho D(\rho)$ as $\rho \to 0$, Obtained from the Boltzmann, Average Scatterer, and Repeated Ring Approximations, and from Simulations

Model	Boltzmann	Average scatterer	Ring	Simulation
Rotator $(\gamma = 1,\ \rho_R = \rho_L = 2\rho_B)$	0.417	0.299	0.361	0.38(2)
Mirror $(\alpha = \beta = \gamma = \frac{1}{3},\ \rho_B = 0)$	0.5	0.348	0.317	0.318
Diamond	0.15	0.10	0.102	0.084
Hexagon A	0.096	0.077	0.077	0.083
Hexagon B	0.115	0.068	0.076	0.049
Triangle	0.105	0.077	0.079	0.068

average scatterer to which the result (6.2) is applied. Let $C_a = \rho_a / \rho$ with $\sum_a C_a = 1$ be the fraction of scatterers of type a. Then the collision matrix $\bar{T}$ of the average scatterer is defined as

$$\bar{T} = \sum_a C_a T_a \qquad (6.6)$$

If we restrict ourselves to models with equal concentrations ($C_R = C_L = C$) of right and left scatterers (rotators in Fig. 1a; mirrors in Fig. 1b), then the average scatterer is described by $\bar{T}$ of (2.9) with average transition probabilities,

$$\bar{\alpha} = 2\alpha C; \qquad \bar{\beta} = 2\beta C + C_B; \qquad \bar{\gamma} = (\delta + \gamma) C \qquad (6.7)$$

where $\delta = 0$ for the mirror model. For the simulation of Fig. 3 this yields $\bar{\alpha} = \bar{\beta} = 1/3$ and $\bar{\gamma} = 1/6$. This average scatterer is identical to the point scatterer of Section 2, and the prediction of the average scatterer approximation coincides with the solid line in Fig. 3. Although this approximation gives only a rough estimate of the actual density dependence, it is still both qualitatively and quantitatively much better than the Boltzmann approximation. The resulting diffusion coefficient for $\rho \to 0$ is also listed in Table I.

For the rotator model, defined in Fig. 1a, simulations of the diffusion coefficient were done in ref. 9 for a random mixture of deterministic rotators ($\gamma = 1$) and reflectors with composition $\rho_R = \rho_L = 2\rho_B = \frac{2}{5}\rho$. The simulated diffusion coefficient $\rho D = 0.38 \pm 0.02$ is listed in Table I. With the restriction to equal concentrations $C_R = C_L = C$ the diffusion coefficient in the repeated ring approximation is given by $D = (2\lambda_1)^{-1}$ with

$$\lambda_1 = 2\gamma\rho \left(2 \, \mathrm{Re} \, \frac{C}{1 + \eta_{R1} y} + C_B \right) \qquad (6.8)$$

The quantity y is the positive solution of (4.17), i.e.,

$$\frac{y}{y + \eta_{R2}} - 2 \, \mathrm{Re} \, \frac{1}{1 + \eta_{R1} y} = \frac{C_B}{C} \qquad (6.9)$$

where η_{R1} and η_{R2} can be obtained from (4.16) and (A.2). For the model parameter of the simulations ($C = 2C_B = 2/5$ and $\gamma = 1$) the solution of (6.9) is $y = \sqrt{3}$. The resulting diffusion coefficient in the repeated ring approximation, $\rho D = (5/24) \sqrt{3} \simeq 0.361$, is also listed in Table I. It agrees well with the simulation result 0.38 ± 0.02 within error bars. The

corresponding Boltzmann approximation, $\rho D^0 \simeq 0.42$, and the average scatterer approximation, $\rho D \simeq 0.30$, which follows from (6.7) with $\bar{\alpha} = 0$, $\bar{\beta} = C_B = 1/5$, and $\bar{\gamma} = C = 2/5$, give very poor theoretical predictions.

6.3. Extended Scatterers

In Fig. 2 of Section 2 we introduced Lorentz lattice gases with finite-size scatterers on square or triangular lattices, and we measured the mean square displacements on these lattices with the help of computer simulations. For the diamond model additional low-density simulations were carried out on the corresponding Cayley tree. The results are listed in Table I and compared with various theoretical results, to be discussed below. The diffusion coefficient is always given by $D = \mathrm{Re}(2\lambda_1)^{-1}$.

In the *repeated ring approximation* the eigenvalues can be obtained from (4.15) with ρ_a replaced by ρ [see below (4.17)]. This expression contains the quantity y, which is the positive root of (4.17). For the *diamond model* the y equation reduces to a quartic equation,

$$\mathrm{Re}\,\frac{4}{1 + \eta_{11}\,y} = \frac{2y}{y + 2} + \frac{y}{y + \frac{1}{2}} - \frac{2}{1 + \frac{1}{2}y} \tag{6.10}$$

with $\eta_{11} = (4 - 3i)/5$ from (4.16) and (B.2). Its solution is $y \simeq 2.5141$. The diffusion coefficient for $\rho \to 0$ follows from (4.14) as

$$\rho D = \frac{1}{4y}\left(\frac{1}{1 + \frac{1}{2}y} + 2\,\mathrm{Re}\,\frac{1}{1 + \eta_{11}\,y}\right)^{-1} \tag{6.11}$$

Its numerical value is listed in Table I, together with the Boltzmann approximation, obtained from (6.11) by setting $y = 1$. It accounts for about 70% of the difference between the simulations and the Boltzmann approximation.

In the *hexagon model A* of Fig. 2c one obtains the y equation in the form

$$\mathrm{Re}\left(\frac{8y}{y + \eta_{12}} - \frac{4}{1 + \eta_{11}\,y} - \frac{4}{1 + \eta_{12}^*\,y}\right) = \frac{5}{1 + \frac{2}{3}y} + \frac{2}{1 + \frac{3}{2}y} - \frac{2y}{y + \frac{2}{3}} \tag{6.12}$$

with $\eta_{11} = 1/\eta_{12}^* = (24 - i5\sqrt{3})/31$ and solution $y \simeq 1.6246$. The diffusion coefficient becomes

$$\rho D = \frac{1}{4y}\left[\frac{1}{1 + \frac{2}{3}y} + \mathrm{Re}\left(\frac{2}{1 + \eta_{11}\,y} + \frac{2}{1 + \eta_{12}\,y}\right)\right]^{-1} \tag{6.13}$$

The Boltzmann value ρD^0 [obtained from (6.13) with $y = 1$] is about 16% higher than the simulation value, while the repeated ring approximation gives a value about 7% lower. The deviations in model A do not follow the general trends of all other models discussed in the paper. This is caused by the large probability (2/5 in a binary collision) that the particle will recollide with the same scatterer in the subsequent time step, whereas this probability is zero in all other models, as discussed in ref. 7.

For the *hexagon model B* of Fig. 2d the y equation is

$$\text{Re} \frac{4}{1 + \eta_{11}\, y} = \frac{6y}{y + 1} - \frac{2}{1 + \frac{1}{5}y} - \frac{2}{1 + \frac{1}{2}y} - \frac{1}{1 + 2y} \tag{6.14}$$

with $\eta_{11} = (5 - i6\sqrt{3})/19$ and solution $y \simeq 2.2024$. The diffusion coefficient becomes

$$\rho D = \frac{1}{4y} \left(\frac{1}{1 + \frac{1}{5}y} + \text{Re}\, \frac{2}{1 + \eta_{11}\, y} \right)^{-1} \tag{6.15}$$

This diffusion coefficient is about 55% larger than the simulations and accounts for only 60% of the deviation from the Boltzmann value.

For the *triangle model* of Fig. 2b the y equation is

$$\text{Re} \left(\frac{1}{1 + \eta_{01}\, y} + \frac{1}{1 + \eta_{11}\, y} - \frac{y}{y + \eta_{02}} \right) = \frac{y}{y + \frac{5}{3}} - \frac{1}{1 + y} \tag{6.16}$$

with $\eta_{11} = (13 - i8\sqrt{3})/19$, $\eta_{01} = (13 - i4\sqrt{3})/31$, $\eta_{02} = (15 - i4\sqrt{3})/21$, and solution $y \simeq 1.8125$, and diffusion coefficient

$$\rho D = \frac{1}{8y} \left(\text{Re}\, \frac{1}{1 + \eta_{11}\, y} + \text{Re}\, \frac{1}{1 + \eta_{01}\, y} \right)^{-1} \tag{6.17}$$

This value accounts for about 70% of the difference between Boltzmann and simulation values.

In summary, the repeated ring approximation gives a very *good* prediction for the diffusion coefficient in the models with mixed point scatterers, and *poor* predictions for models with excluded volume effects.

Finally we apply the average scatterer approximation to the extended scatterers. In the low-density limit or on a Cayley tree the M different impact parameters, labeled a in (3.8), can be considered as different point scatterers, so that the mean free path is $\bar{l} = (\rho M)^{-1}$, which is to be used in (6.1). In the diamond model of Fig. 2a the labels for the impact parameters are $a = 0, 1, 3$ and $M = 3$; in model A of Fig. 2c the labels are $a = 0, 1, 2, 4, 5$ and $M = 5$; in model B of Fig. 2d the labels are $a = 0, 1, 5$ and $M = 3$;

in the triangle model of Fig. 2b the labels are $a = 0$, 1, 4, 5 and $M = 4$. The collision matrix $\bar{T}$ in (6.6) for the average scatterer is given by $\bar{T} = (\sum_a T_a)/M$ with T_a given in (B.1), (B.3), (B.5), and (B.8).

The average transition probabilities [compare (6.7)] are, for the *diamond model*,

$$\bar{\alpha} = \bar{\gamma} = 2/9; \qquad \bar{\beta} = 1/3$$

The analog of the square lattice point scatterer (2.9) on a triangular lattice has transmission probability α, a reflection probability γ for 60° angles and δ for 120° angles, with $\alpha + \beta + 2\gamma + 2\delta = 1$. With these definitions the parameters for the average scatterer approximation are, for the *hexagon model A*,

$$\bar{\alpha} = \bar{\gamma} = \bar{\delta} = 4/25; \qquad \bar{\beta} = 1/5$$

for the *hexagon model B*,

$$\bar{\alpha} = 0; \qquad \bar{\beta} = 1/3; \qquad \bar{\gamma} = 1/9; \qquad \bar{\delta} = 2/9$$

and for the *triangle model*,

$$\bar{\alpha} = \bar{\gamma} = 1/8; \qquad \bar{\beta} = 1/4; \qquad \bar{\delta} = 3/16$$

Applying the linear interpolation formula (6.2) to the average extended scatterers and solving x from (5.2) or y from (5.4) yields the results of Table I for the average scatterer approximation. We conclude that the repeated ring and the average scatterer approximation give equally poor predictions for the diffusion coefficient if excluded volume effects are present.

7. DISCUSSION

The main results of this paper are:

1. The analytic solution (4.15)–(4.17) of the repeated ring approximation for small densities on general lattices (square, triangular) and for general types of scatterers (mixed point scatterers, extended scatterers).

2. The demonstration in Section 5 that in the special case of *identical point* scatterers the approximate repeated ring approximation gives the exact, non-mean-field result that was obtained recently by van Beijeren and Ernst[5] by an exact enumeration method of trajectories on Cayley trees.

3. The computer simulations of the diffusion coefficients in Section 6, which demonstrate the total failure of the Boltzmann equation in predicting the low-density diffusion coefficient. For identical point scatterers, the simulations compare very well (see Fig. 3) for all densities with the linear

interpolation formula of ref. 5. For mixed point scatterers the predictions of the repeated ring theory agree well with the computer simulations, both for mirror and for chiral models in the low-density limit.

4. In models with hard-core scatterers the repeated ring approximation gives a reasonable estimate of the computer-simulated values. The prediction accounts for about 60–70% of the observed difference between simulations and mean field theory.

5. To account for the observed difference between simulations and repeated ring kinetic theory in hard-core systems it seems necessary to evaluate, even in the low-density limit, non-ring-type collision sequences, such as repeated crossings ($abab\cdots$) of the moving particle between two scatterers a and b.

6. An alternative method for obtaining the low-density diffusion coefficient in Lorentz gases with extended scatterers would be to do the exact enumeration of all possible trajectories on the corresponding Cayley tree by computer. The exact enumeration of trajectories containing up to 8 scatterers on a triangular lattice and up to 11 scatterers on a square lattice can be done. The extrapolated results for the diffusion coefficient agree well with the present simulations.[10]

APPENDIX A. MODELS WITH POINT SCATTERERS

In this appendix two Lorentz gas models with a mixture of different types of point scatterers are described and the corresponding collision operators are given explicitly.

A1. Rotator Model

In this model the particle moves on a square lattice with three types of point scatterers with concentration ρ_R, ρ_L, and ρ_B, with $\rho_R + \rho_L + \rho_B = \rho$. The collision rules are illustrated in Fig. 1a. If the particle hits a scatterer of type R (L), it has probabilities α, β, γ, and $\delta = 1-(\alpha+\beta+\gamma)$ of being transmitted, reflected, deflected to the right (left), and deflected to the left (right), respectively. Scatterers of type B are pure reflectors. In the deterministic case ($\alpha = \beta = \delta = 0$), this model reduces to the one introduced by Gunn and Ortuño.[1] The model has rotation symmetry. The binary collision matrix T_a in (2.7) takes the form

$$T_R = (\alpha - 1)\mathbf{1} + \delta\mathscr{D} + \beta\mathscr{D}^2 + \gamma\mathscr{D}^3$$

$$T_L = (\alpha - 1)\mathbf{1} + \gamma\mathscr{D} + \beta\mathscr{D}^2 + \delta\mathscr{D}^3 \qquad (A.1)$$

$$T_B = \mathscr{D}^2 - \mathbf{1}$$

The rotation matrix $\mathscr{D}$ is defined in (2.10). The common set of eigenvectors of the matrices T_a is given in (C.3) of Appendix C. The corresponding eigenvalues $-\tau_{al}$ defined in (3.10) are

$$\tau_{Rl} = \tau_{Ll}^* = 1 - \alpha - \delta \hat{\imath}^l - \beta(-1)^l - \gamma(-\hat{\imath})^l$$

$$\tau_{Bl} = 1 - (-1)^l \tag{A.2}$$

where $\hat{\imath} = (-1)^{1/2}$. The label l is introduced in (3.9).

A2. Mirror Model

In the rotator model the action of a scatterer is defined with respect to the direction of the moving particle. In the mirror model the action is defined with respect to the orientation of mirrors in the lattice. In this model three types of scatterers can occupy the sites of a square lattice: right mirrors (R), left mirrors (L), and reflectors (B). The stochastic collision rules for the mirrors, shown in Fig. 1b, are normalized as $\alpha + \beta + \gamma = 1$. Again the model can be specialized to a deterministic model by setting $\alpha = \beta = 0$. If in addition $\rho_B = 0$, it reduces to the deterministic model introduced by Ruijgrok and Cohen.[3]

This model possesses reflection symmetry. The collision matrix is given by (2.7) with

$$T_R = (\alpha - 1)\mathbf{1} + \beta U_B + \gamma U_R$$

$$T_L = (\alpha - 1)\mathbf{1} + \beta U_B + \gamma U_L \tag{A.3}$$

$$T_B = U_B - \mathbf{1}$$

The matrices U_a are defined as

$$U_R = \mathscr{P}_{01}\mathscr{P}_{23}, \qquad U_L = \mathscr{P}_{03}\mathscr{P}_{12}, \qquad U_B = \mathscr{P}_{02}\mathscr{P}_{13} \tag{A.4}$$

where the permutation operator $\mathscr{P}_{kl}$ interchanges the labels k and l and leaves the other labels invariant. Its eigenvectors are given in (C.8). Here we list the eigenvalues $(-\tau_{al})$ of the collision operators in (A.3):

$$\tau_{a0} = 0, \qquad \tau_{R1} = \tau_{L3} = 2\beta, \qquad \tau_{R2} = \tau_{L2} = 2\gamma$$

$$\tau_{R3} = \tau_{L1} = 2(\beta + \gamma), \qquad \tau_{B1} = \tau_{B3} = 2, \qquad \tau_{B2} = 0 \tag{A.5}$$

Here we have constructed the collision operators for two typical examples of Lorentz models containing several types of scatterers. The method can be easily extended to different types of scatterers and to different lattices.

APPENDIX B. MODELS WITH EXTENDED SCATTERERS

B1. Diamond Model

Diamond-shaped hard scatterers are put randomly on a square lattice (see Fig. 2a). The three possible incoming states of the moving particle ($a = 0$, 1, 3) are indicated with an open arrow; the three possible outgoing states (solid arrows) are equally probable and are independent of the incoming velocity. The collision operator is given by (2.8) with T-matrices

$$T_a = -\mathbf{1} + \tfrac{1}{3} \sum_{k=0,\, k \neq a}^{3} \mathscr{D}^k \tag{B.1}$$

with $a = 0$, 1, 3. The eigenvectors and eigenvalues of the rotation matrices are given in (C.1) of Appendix C. From there one obtains the eigenvalues $-\tau_{al}$ of the collision matrix T_a ($a = 0$, 1, 3) as

$$\tau_{a0} = 0, \qquad \tau_{al} = 1 + \tfrac{1}{3} \hat{\imath}^{al} \tag{B.2}$$

with $l = 1$, 2, 3, which are needed in the body of the paper.

B2. Hexagon Model A

It is the direct analog of the diamond model on the triangular lattice, as illustrated in Fig. 2c. Here hard hexagons are put on a triangular lattice. There are five possible outgoing directions. The only excluded bond is the one connecting the point of impact with the center of the hexagon. The collision operator is again given by (2.8) with the binary collision T-matrices given by

$$T_a = -\mathbf{1} + \tfrac{1}{5} \sum_{k=0,\, k \neq a}^{5} \mathscr{D}^k \tag{B.3}$$

with $a = 0$, 1, 2, 4, 5. The eigenvectors and eigenvalues of the $\mathscr{D}$-matrices are given in (C.1) with $b = 6$, from where it follows at once that

$$\tau_{a0} = 0, \qquad \tau_{al} = 1 + \tfrac{1}{5} \theta^{al} \tag{B.4}$$

with $a = 0$, 1, 2, 4, 5 and $l = 1$, 2, 3, 4, 5. Here $\theta = \exp(\hat{\imath}\pi/3) = \tfrac{1}{2}(1 + \hat{\imath}\sqrt{3})$.

B3. Hexagon Model B

This model is similar to the previous one, except that particles are not allowed to move along the edges of the hexagonal scatterers (see Fig. 2d) and the binary collision matrices T_a are given by

$$T_0 = -\mathbf{1} + \tfrac{1}{3}(\mathscr{D}^2 + \mathscr{D}^3 + \mathscr{D}^4)$$

$$T_1 = -\mathbf{1} + \tfrac{1}{3}(\mathscr{D}^3 + \mathscr{D}^4 + \mathscr{D}^5) \tag{B.5}$$

$$T_5 = -\mathbf{1} + \tfrac{1}{3}(\mathscr{D} + \mathscr{D}^2 + \mathscr{D}^3)$$

The eigenvalues of the matrices T_a follow again from (C.1) with $b = 6$. The result for $l = 0, 1,..., 6$ is

$$\tau_{0l} = 1 - \tfrac{1}{3}[(-)^l + (-\theta)^l + (-\theta^*)^l]$$

$$\tau_{1l} = \tau_{5l}^* = 1 - \tfrac{1}{3}[(-)^l + (-\theta)^l + \theta^{*l}] \tag{B.6}$$

with θ defined below (B.4).

B4. Triangle Model

As in the two previous models, the lattice is triangular. The scatterers are now triangles located at the centers of the unit cells, as illustrated in Fig. 2b. Their positions are denoted by the reciprocal lattice vectors $\mathbf{c}_i$ ($i = 0, 1,..., 5$). No sites are excluded to the moving particle, but the edges of the triangles are. The density $\rho = \langle s(\mathbf{r} + \mathbf{c}_i) \rangle$ denotes the fraction of unit cells occupied by a triangle. Figure 2b shows the collision rules for a single scatterer, which admit four outgoing velocity states. The collision operator has the form

$$I_{ij}(\mathbf{r} \,|\, \mathbf{s}) = \sum_a s(\mathbf{r} + \mathbf{c}_{i+a}^*) T_{aij} \tag{B.7}$$

with $a = 0, 1, 4, 5$. The binary collision T-matrices are

$$T_a = -\mathbf{1} + \tfrac{1}{4} \sum_{k=0}^{5}{}^* \mathscr{D}^k \tag{B.8}$$

with the constraint (*) on the sum $k \neq a, a + 1$. The eigenvalues and eigenvectors of the $\mathscr{D}$-matrices are given in (C.1) with $b = 6$, from where it follows at once that

$$\tau_{a0} = 0, \qquad \tau_{al} = 1 + \tfrac{1}{4}(\theta^{al} + \theta^{(a+1)l}) \tag{B.9}$$

with θ defined below (B.4) and with $a = 0, 1, 4, 5$ and $l = 1, 2, 3, 4, 5$.

In ref. 7 more precise definitions of the T-matrices are given, which are required at finite densities where multiple collisions can occur.

APPENDIX C. EIGENVALUES AND EIGENFUNCTIONS

The probability distribution function for finding a scatterer of a certain type at site $\mathbf{r}$ is a site-independent quantity and therefore has the same discrete symmetry as the underlying space lattice. The scatterers, defined for the different models of this paper (see Appendixes A and B), are described by transition probabilities which either have rotation symmetry or reflection symmetry or both.

Consequently the transition matrices T_a defined in Appendixes A and B, the Boltzmann collision operator Λ^0 in (3.1), the repeated ring collision operator Λ in (3.5) or (3.8), and the ring operator R in (3.6) are $b \times b$ matrices with either rotation or reflection symmetries, or both. These matrices commute with the matrices representing rotations or reflections and have common eigenvectors $|\varphi_l\rangle$ $(l = 0, 1, 2, ..., b-1)$.

For the matrix $\mathcal{D}$, representing the basic rotation over $2\pi/b$ in the counterclockwise direction, one has

$$(\mathcal{D}\varphi_l)_j = \varphi_{l,j+1} \equiv d_l \varphi_{lj}$$

$$d_l = \exp(2l\pi\hat{\imath}/b) \qquad (l = 0, 1, 2, ..., b-1) \qquad \text{(C.1)}$$

$$\varphi_{lj} = \exp(2jl\pi\hat{\imath}/b) \qquad (j = 0, 1, ..., b-1)$$

where b is the coordination number in two-dimensional lattices, $\hat{\imath} = (-1)^{1/2}$, and $\langle \varphi_l | \varphi_{l'} \rangle = \delta_{ll'}$, according to the inner product in (2.4).

In the analysis of Section 4 it will also be convenient to have a representation of the eigenvectors $|\varphi_l\rangle$ in the basis $\{|V_k\rangle, |V_k^2\rangle; k = 0, 1, ..., b/2 - 1\}$ with components

$$V_{kj} = \delta_{jk} - \delta_{j,k+b/2} \qquad (j = 0, 1, ..., b-1) \qquad \text{(C.2)}$$

Then, for *square lattices* with *rotational symmetry* $(b = 4)$, the eigenvalues are $d_l = \hat{\imath}^l$ $(l = 0, 1, 2, 3)$ and the eigenvectors are

$$|\varphi_0\rangle = (1, 1, 1, 1) = |V_0^2\rangle + |V_1^2\rangle$$

$$|\varphi_1\rangle = |\varphi_3^*\rangle = (1, \hat{\imath}, -1, -\hat{\imath}) = |V_0\rangle + \hat{\imath}|V_1\rangle \qquad \text{(C.3)}$$

$$|\varphi_2\rangle = (1, -1, 1, -1) = |V_0^2\rangle - |V_1^2\rangle$$

with the inverse relations

$$|V_0\rangle = \frac{1}{2}(|\varphi_1\rangle + |\varphi_3\rangle), \qquad |V_1\rangle = \frac{1}{2\hat{\imath}}(|\varphi_1\rangle - |\varphi_3\rangle)$$

$$\text{(C.4)}$$

$$|V_0^2\rangle = \frac{1}{2}(|\varphi_0\rangle + |\varphi_2\rangle), \qquad |V_1^2\rangle = \frac{1}{2}(|\varphi_0\rangle - |\varphi_2\rangle)$$

Similarly it follows for the *triangular lattice* with *rotational symmetry* ($b = 6$) that the eigenvalues are $d_l = \theta^l$ ($l = 0, 1,..., 5$) with $\theta = \frac{1}{2}(1 + i\sqrt{3})$ and the eigenvectors are

$$
\begin{aligned}
|\varphi_0\rangle &= |V_0^2\rangle + |V_1^2\rangle + |V_2^2\rangle \\
|\varphi_1\rangle &= |\varphi_5^*\rangle = |V_0\rangle + \theta |V_1\rangle - \theta^* |V_2\rangle \\
|\varphi_2\rangle &= |\varphi_4^*\rangle = |V_0^2\rangle - \theta^* |V_1^2\rangle - \theta |V_2^2\rangle \\
|\varphi_3\rangle &= |V_0\rangle - |V_1\rangle + |V_2\rangle
\end{aligned}
\tag{C.5}
$$

with the inverse relations

$$
\begin{aligned}
|V_0\rangle &= \tfrac{1}{3}(|\varphi_1\rangle + |\varphi_3\rangle + |\varphi_5\rangle) \\
|V_1\rangle &= \tfrac{1}{3}(\theta^* |\varphi_1\rangle - |\varphi_3\rangle + \theta |\varphi_5\rangle) \\
|V_2\rangle &= \tfrac{1}{3}(-\theta |\varphi_1\rangle + |\varphi_3\rangle - \theta^* |\varphi_5\rangle) \\
|V_0^2\rangle &= \tfrac{1}{3}(|\varphi_0\rangle + |\varphi_2\rangle + |\varphi_4\rangle) \\
|V_1^2\rangle &= \tfrac{1}{3}(|\varphi_0\rangle - \theta |\varphi_2\rangle - \theta^* |\varphi_4\rangle) \\
|V_2^2\rangle &= \tfrac{1}{3}(|\varphi_0\rangle - \theta^* |\varphi_2\rangle - \theta |\varphi_4\rangle)
\end{aligned}
\tag{C.6}
$$

As far as *reflection symmetries* are concerned, the eigenvectors are only illustrated for the *square lattice*. The mirror planes are oriented under angles of $\pm \pi/4$. Then the matrices T_a, Λ^0, Λ, and R commute, with the following matrices representing the symmetry operations:

$$
U_R = \mathcal{P}_{01}\mathcal{P}_{12}, \qquad U_L = \mathcal{P}_{03}\mathcal{P}_{12}, \qquad U_B = \mathcal{P}_{02}\mathcal{P}_{13}
\tag{C.7}
$$

where the permutation operators $\mathcal{P}_{ij}$ interchanges the labels (components) i and j. The eigenvectors are

$$
\begin{aligned}
|\varphi_0\rangle &= (1, 1, 1, 1) = |V_0^2\rangle + |V_1^2\rangle \\
|\varphi_1\rangle &= (1, 1, -1, -1) = |V_0\rangle + |V_1\rangle \\
|\varphi_2\rangle &= (1, -1, 1, -1) = |V_0^2\rangle - |V_1^2\rangle \\
|\varphi_3\rangle &= (1, -1, -1, 1) = |V_0\rangle - |V_1\rangle
\end{aligned}
\tag{C.8}
$$

with eigenvalues

$$
\begin{aligned}
u_{R0} &= u_{R1} = -u_{R2} = -u_{R3} = 1 \\
u_{L0} &= -u_{L1} = -u_{L2} = u_{L3} = 1 \\
u_{B0} &= -u_{B1} = u_{B2} = -u_{B3} = 1
\end{aligned}
\tag{C.9}
$$

The inverse relations are

$$|V_0\rangle = \tfrac{1}{2}(|\varphi_1\rangle + |\varphi_3\rangle), \qquad |V_1\rangle = \tfrac{1}{2}(|\varphi_1\rangle - |\varphi_3\rangle)$$
$$|V_0^2\rangle = \tfrac{1}{2}(|\varphi_0\rangle + |\varphi_2\rangle), \qquad |V_1^2\rangle = \tfrac{1}{2}(|\varphi_0\rangle - |\varphi_2\rangle) \qquad \text{(C.10)}$$

ACKNOWLEDGMENTS

REFERENCES

1. J. M. F. Gunn and M. Ortuño, *J. Phys. A: Math. Gen.* **18**:L1035 (1985).
2. G. A. van Velzen and M. H. Ernst, *J. Phys. A: Math. Gen.* **22**:4611 (1989).
3. Th. W. Ruijgrok and E. G. D. Cohen, *Phys. Lett. A* **123**:515 (1988); G. A. van Velzen, *J. Phys. A: Math. Gen.* **24**:807 (1991).
4. M. H. Ernst, G. A. van Velzen, and P. M. Binder, *Phys. Rev. A* **39**:4327 (1989).
5. H. van Beijeren and M. H. Ernst, *J. Stat. Phys.*, to appear.
6. D. Frenkel, F. van Luijn, and P. M. Binder, *Europhys. Lett.* **20**:7 (1992).
7. A. J. H. Ossendrijver, A. Santos, and M. H. Ernst, *Physica A*, to be published.
8. G. A. van Velzen, *J. Phys. A: Math. Gen.* **23**:4953 (1990).
9. G. A. van Velzen, *J. Phys. A: Math. Gen.* **24**:787 (1991).
10. A. J. H. Ossendrijver and M. H. Ernst, *J. Stat. Phys.*, to be published.